MOLECULAR AND CELLULAR BIOLOGY, Jan. 2004, p. 697–707 Vol. 24, No. 2
0270-7306/04/$08.00+0 DOI: 10.1128/MCB.24.2.697–707.2004
Copyright © 2004, American Society for Microbiology. All Rights Reserved.

Structural Features of Transcription Factor IIIA Bound to a Nucleosome in Solution

Joseph M. Vitolo,†‡ Zungyoon Yang,† Ravi Basavappa, and Jeffrey J. Hayes*

Department of Biochemistry and Biophysics, University of Rochester Medical Center, Rochester, New York 14625

Received 16 July 2003/Returned for modification 23 September 2003/Accepted 14 October 2003

Assembly of a DNA fragment containing a *Xenopus borealis* somatic-type 5S RNA gene into a nucleosome greatly restricts binding of the 5S gene-specific transcription factor IIIA (TFIIIA) to the 5S internal promoter. However, TFIIIA binds with high affinity to 5S nucleosomes lacking the N-terminal tail domains of the core histones or to nucleosomes in which these domains are hyperacetylated. The degree to which tail acetylation or removal improves TFIIIA binding cannot be simply explained by a commensurate change in the general accessibility of nucleosomal DNA. In order to investigate the molecular basis of how TFIIIA binds to the nucleosome and to ascertain if binding involves all nine zinc fingers and/or displacement of histone-DNA interactions, we examined the TFIIIA-nucleosome complex by hydroxyl radical footprinting and site-directed protein-DNA cross-linking. Our data reveal that the first six fingers of TFIIIA bind and displace approximately 20 bp of histone-DNA interactions at the periphery of the nucleosome, while binding of fingers 7 to 9 appears to overlap with histone-DNA interactions. Molecular modeling based on these results and the crystal structures of a nucleosome core and a TFIIIA-DNA cocomplex yields a precise picture of the ternary complex and a potentially important intermediate in the transition from naïve chromatin structure to productive polymerase III transcription complex.

The assembly of DNA into the basic subunit of chromatin, the nucleosome, severely restricts the activity of most sequence-specific DNA binding factors. This is due to constraints arising from the intimate association of the DNA with histone proteins and the severe DNA bending and changes in helical periodicity that occur upon nucleosome formation (18, 26, 49). However, nucleosomes are dynamic structures, in rapid equilibrium with states in which the DNA is partially unwound and as accessible to DNA binding proteins as naked DNA (32). Thus, DNA binding transcription factors compete directly with histones for binding to nucleosomal DNA (32). Importantly, Widom and colleagues have demonstrated that this simple competition between histones and *trans*-acting factors leads to inherent cooperativity in the binding of otherwise unrelated factors and appears to be operative in vivo (28, 33).

Given the apparent role of chromatin structure in the developmental regulation of the 5S rRNA gene system from *Xenopus* (1, 3, 48), DNA fragments containing these genes have been useful model systems for investigation of the interplay between the binding of histones and transcription factors to the same DNA (35, 46). DNA fragments containing 5S genes harbor robust nucleosome positioning elements that direct the binding of histones upon reconstitution in vitro (10, 38). Moreover, the initial event in transcriptional activation of the 5S gene family involves binding of the 5S-specific transcription factor IIIA (TFIIIA) to an internal promoter (internal control region) (9). TFIIIA is a nine-zinc-finger protein (4, 27) which binds in a complex fashion along the entire length of the ~50-bp internal promoter in three structurally distinct modules (39, 44). A DNA fragment containing a *Xenopus borealis* somatic-type 5S gene assembles into positioned nucleosomes upon reconstitution with purified core histones (16, 35, 40). Hydroxyl radical footprinting has shown that strong core histone-DNA contacts extend from ~−75 to ~+70 within the 5S sequence, with weaker interactions detected up to 10 to 20 bp to either side of this region (16, 40). Thus histone-DNA contacts exist throughout the majority of the 5S internal promoter, including the +80 through +90 region, which contains the most energetically important contacts for TFIIIA binding (Fig. 1) (13, 15, 36). Accordingly, assembly of the 5S DNA fragment into nucleosomes severely restricts TFIIIA binding to the 5S internal promoter (17, 40). However, TFIIIA binds with relatively high affinity to 5S nucleosomes in which the histone tail domains are hyperacetylated or have been removed (23, 43).

The mechanism by which acetylation or removal of the core histone tails enhances TFIIIA binding is unclear. Both of these alterations have only marginal effects on the extent of histone-DNA contacts within nucleosomes or probability of site exposure for nucleosomal DNA (2, 6, 12, 31). Moreover, the details of the interaction between the 5S nucleosome and TFIIIA have not been defined. For example, do all nine zinc fingers of this modular protein bind DNA within the nucleosome? To what extent are histone-DNA interactions disrupted upon TFIIIA binding? Previous studies examining the solution structure of the TFIIIA-5S nucleosome complex using DNase I protection assays were unable to discriminate between TFIIIA Zn-finger–DNA interactions and histone-DNA interactions in this ternary complex (23, 35). However, hydroxyl radical footprinting has been used to distinguish between the binding of individual zinc fingers of TFIIIA to 5S DNA (13, 44) and to precisely map histone-DNA interactions (16), suggesting that

* Corresponding author. Mailing address: Department of Biochemistry and Biophysics, University of Rochester Medical Center, Rochester, NY 14625. Phone: (585) 273-4887. Fax: (585) 271-2683. E-mail: jjhs@mai.rochester.edu.
† J.M.V. and Z.Y. contributed equally to this work.
‡ Present address: NIH, NIDCR, GTTB, Bethesda, MD 20892.

Downloaded from http://mcb.asm.org/ on July 23, 2019 by guest

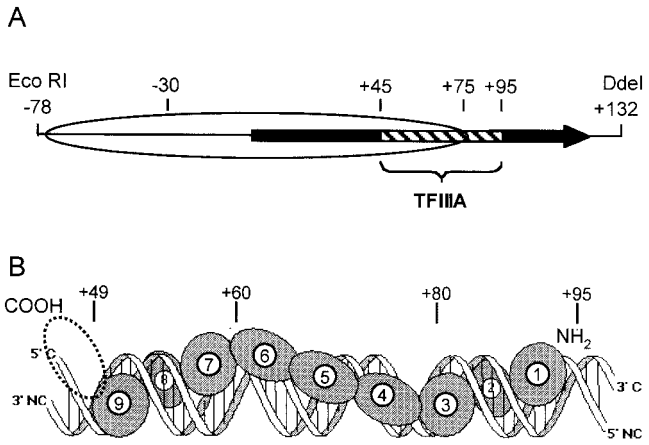

FIG. 1. A DNA fragment containing a *Xenopus* somatic-type 5S RNA gene. (A) Diagram showing the approximate location of the main nucleosome translational position. The oval corresponds to the 147-bp nucleosome core region, but note that histone-DNA interactions are detected outside of this region (16, 40). The location of the 5S gene (black arrow) and the internal promoter where TFIIIA binds (hatched box) are shown. Numbers are with respect to the start site of transcription of the 5S gene at +1. (B) Schematic of the proposed TFIIIA-DNA complex, based on references 7, 15, and 29. The 4-kDa COOH-terminal transcription activation domain is represented as a dotted oval.

this method may reveal such structural details within the TFIIIA-nucleosome complex.

To elucidate structural details of TFIIIA bound to a 5S nucleosome, we performed quantitative hydroxyl radical footprinting of the TFIIIA-nucleosome complex. Comparisons to the naked DNA-TFIIIA complex and the nucleosome cleavage pattern allowed a precise determination of the location of histone-DNA interactions and the interactions of TFIIIA zinc fingers within the triple complex. These data, coupled with protein-DNA cross-linking studies and molecular modeling, allow the construction of a well-defined model for how this transcription factor binds to the 5S nucleosome, revealing an important initial intermediate in the process of histone eviction and formation of a competent preinitiation complex.

MATERIALS AND METHODS

DNA fragment, histones, and nucleosome reconstitution. A 215-bp DNA fragment containing a somatic-type 5S rRNA gene from *X. borealis* was obtained from the plasmid XP-10 by digestion with *Eco*RI and *Dde*I (43). Reconstitution of this template with core histones resulted in the majority of nucleosomes generated adopting translational positions near the 5′ end of the fragment (Fig. 1) (16). The fragment was radiolabeled at the 5′ *Eco*RI site with [γ-^{32}P]ATP and T4 polynucleotide kinase by standard methods (43). Histones were prepared from chicken erythrocyte nuclei as described previously (37). Tailless histones for reconstitution were prepared by treatment of stripped chromatin or reconstituted nucleosomes with trypsin-linked agarose beads as described elsewhere (41, 43). Nucleosomes were reconstituted with radioactively labeled 5S DNA together with unlabeled sheared calf thymus DNA via salt-gradient dialysis (14).

TFIIIA binding assays. TFIIIA was prepared from *Xenopus* oocytes (39) or overexpressed in bacterial cells and purified as described previously (8). TFIIIA prepared by either method behaved identically in nucleosome binding assays. TFIIIA binding reactions were carried out with 10 μl of the reconstituted histone-DNA complexes (~250 ng of total DNA; ~25 fmol of total 5S DNA) in binding buffer (50 mM NH_4Cl, 10 mM HEPES [pH 7.4], 5 mM $MgCl_2$, 20 μM $ZnCl_2$, 5 mM dithiothreitol, 0.02% Nonidet P-40, 20 μg of bovine serum albumin/ml, and 100 ng of calf thymus DNA) in a final volume of 13 μl. Complexes were incubated with purified TFIIIA as indicated in the figure legends for 1 h at 23°C and then loaded directly onto 0.7% agarose nucleoprotein gels containing 0.5× TB buffer (45 mM Tris borate [pH 8.3]) and electrophoresed for ~2 h at 20 mA in the same buffer. EDTA was omitted from all buffers.

Hydroxyl radical footprinting analysis of the triple complex. Nucleosomes were reconstituted with either wild-type or trypsinized core histones as described above. The amount of TFIIIA required to bind the nucleosome on a preparative scale was determined by careful stepwise titration and analysis on 0.7% agarose nucleoprotein gels (17, 23). Typically, TFIIIA binding reaction mixtures were prepared as described above but scaled up by a factor of 10 to a reaction volume of 130 μl for footprinting studies. The samples were subjected to hydroxyl radical digestion by mixing 6.5 μl of 0.5 mM Fe(II)-EDTA and 6.5 μl of 1 mM sodium ascorbate together on the sides of the tube, then adding 6.5 μl of 0.12% hydrogen peroxide to the drop and immediately mixing these reagents with the binding reaction mixture. The digestion was allowed to proceed for 2 min, and then reactions were quenched by the addition of glycerol to a final concentration of 5% prior to loading onto 0.7% agarose preparative gels (17, 43). The gels were electrophoresed at 20 mA for 2 h, and then the complexes were identified by autoradiography of the wet gel. Bands corresponding to free DNA, TFIIIA/DNA complex, wild-type nucleosome, unbound trypsinized nucleosomes, and the ternary complex containing 5S DNA/trypsinized core histones/TFIIIA were identified and excised. Gel slices were placed into Spin-X tubes, placed at −80°C for 30 min, and then spun at 13,000 rpm in a Brinkman microfuge for 30 min to elute the protein and DNA. The gel plugs were reextracted with an equal volume of Tris-EDTA buffer containing 0.2% sodium dodecyl sulfate (SDS), and then the two eluates were combined. The DNA was precipitated twice and then analyzed by sequencing gel electrophoresis and phosporimager quantitation of the dried gels (43).

Cross-linking of tailless 5S nucleosomes containing APB-modified H2A. Dimers containing the mutant H2A-A12C or H2A-A45C (in which alanine 12 or 45 is changed to cysteine, respectively) were prepared and then modified with the cross-linking agent 4-azidophenacylbromide (APB; Sigma) as described previously (24). Nucleosomes containing these proteins were reconstituted as described above, except that concentrations of histones and DNA were increased fivefold and the total volume of the reconstitution increased 10-fold (50-fold more material reconstituted). After reconstitution, the material was concentrated 10-fold by using a filtration concentrator (Millipore) (52). A portion of the nucleosomes were irradiated for 30 s at 365 nm to induce protein-DNA cross-linking before treatment with the trypsin-agarose resin to remove core histone tails as described above. The proteolysis was checked by SDS-polyacrylamide gel electrophoresis (SDS-PAGE) of a portion of the sample, and the cross-linked tailless nucleosomes were purified by sucrose-gradient centrifugation. Cross-linked, tailless nucleosomes were then incubated with TFIIIA, and bound and unbound complexes were separated on preparative 0.7% agarose nucleoprotein gels. DNA was purified from each band in the gel and loaded onto an SDS–6% PAGE, and the gel was electrophoresed at 100 V for 14 h to analyze the amount of cross-link species in each band (24). Alternatively, the reconstituted (unirradiated) nucleosomes containing H2A-A12C-APB were treated directly with trypsin-agarose beads to remove core histone tails. These nucleosomes were purified by sucrose gradients and then incubated without or with TFIIIA and complexes separated on agarose nucleoprotein gels. After electrophoresis, the gel was irradiated for 30 s at 365 nm to induce cross-linking, and the amount of H2A cross-linked to labeled DNA was determined by electrophoresis on SDS-PAGE as described above.

Molecular modeling of the TFIIIA-nucleosome complex. The Nolte et al. structure (29), which contains the first six zinc-finger domains in complex with 5S DNA, was used as the starting point to generate a model of the TFIIIA/DNA complex with all nine zinc-finger domains. The model of the 5S DNA was extended using the program SYBYL (SYBYL Molecular Modeling System; Tripos, Inc., St. Louis, Mo.) to include the binding sites for zinc fingers 7 to 9. To model the position of zinc fingers 7 to 9, the rotation and translation operators that superimpose zinc-finger binding sites 1 to 3 onto zinc-finger binding sites 7 to 9 were found using the program O (20). The same operators then were applied to zinc fingers 1 to 3 to generate the model for fingers 7 to 9. The nine-zinc-finger-containing model was then energy minimized using the program CNS (5). To prepare the TFIIIA/nucleosome complex model, the TFIIIA model was connected to the nucleosome model using the corresponding base positions of 116 in the Luger et al. structure (26) and position 40 in the 5S RNA gene. The resulting complex was energy minimized using the CNS program.

RESULTS

Previous work has demonstrated that while binding of TFIIIA to a nucleosome containing an *X. borealis* somatic-type

Downloaded from http://mcb.asm.org/ on July 23, 2019 by guest

5S gene and native core histones is severely restricted, TFIIIA binds to a 5S nucleosome lacking the core histone tail domains with an affinity approaching that for binding naked 5S DNA (17, 23, 43). To determine the extent of TFIIIA-DNA and histone-DNA interactions in the TFIIIA/5S DNA/core histone ternary complex, native and tailless 5S nucleosomes and naked 5S DNA were incubated with TFIIIA in binding buffer, and then complexes were treated with hydroxyl radicals and separated on preparative nucleoprotein gels. Radiolabeled DNAs from individual species were isolated from these gels, and the cleavage patterns were analyzed by sequencing gel electrophoresis and phosphorimagery (see Materials and Methods) (Fig. 2A). Pixel density was integrated from top to bottom through each lane, and the data were plotted versus linear position along the gel (Fig. 2B). Quantitative comparison of the nucleosome and naked DNA showed that the extreme downstream edge of the nucleosome footprint extends to approximately +90 (Fig. 2C), as expected from previous analyses (16, 40). Interestingly, the footprints of the tailless and native nucleosomes were nearly identical, with only small differences detected near the very edge of the footprint (Fig. 2B), consistent with previous results (2, 12). Note that in these experiments the radioactive label is incorporated at the 5′ end of the noncoding (top) strand in the 5S DNA fragment (Fig. 1A).

The nine zinc fingers of TFIIIA bind in a complex fashion along the entire length of the ~50-bp internal promoter in three structurally distinct modules (Fig. 1B) (39, 44). Fingers 1 to 3 form a three-finger unit similar in gross detail to the interaction of zif268 with DNA (29, 30, 45, 51). These fingers lie primarily within the major groove at the 3′-most end of the promoter and account for the continuous zone of protection in the hydroxyl radical footprint in the region +79 to +90 (Fig. 2B and C, top). In contrast, fingers 4 to 6 lie along one side of the DNA, crossing over major and minor grooves in the center of the promoter (7, 13, 15, 29) and resulting in deep protections and peaks in cleavage in the region from +79 to approximately +58. Finally, fingers 7 to 9 likely wrap around the DNA in a manner similar to fingers 1 to 3 at the 5′-most end of the internal promoter, contacting positions +59 to +49 (7, 13, 15). Importantly, the residues beyond finger 9, including the C-terminal transcription activation domain, extend the hydroxyl radical footprint to approximately position +40 on this strand (Fig. 2C, top).

To assess the interactions of TFIIIA with DNA within the nucleosome, the hydroxyl radical cleavage pattern of the ternary complex was compared to the cleavage patterns of TFIIIA bound to naked 5S DNA and the nucleosome alone. Overlays of the TFIIIA-DNA pattern on the naked DNA cleavage pattern clearly showed that the protein protected bases from approximately +40 to +95 within the 5S top (noncoding) strand from cleavage by hydroxyl radicals (Fig. 3A), consistent with earlier results (13, 44). Comparison of the footprint of the ternary complex to the TFIIIA-DNA and nucleosome patterns (Fig. 3) revealed three distinct regions of structure within the TFIIIA-nucleosome complex. The 5′-most region of the ternary complex has a hydroxyl radical cleavage pattern nearly indistinguishable from that of the nucleosome alone, extending from the upstream region to approximately position +45 (Fig. 3). In addition, the 3′-most region of the complex, from approximately position +58 to the downstream end of the fragment, has features identical to those found within the TFIIIA-DNA complex (Fig. 3). Notably, in between these two regions lies a transition zone which has features that appear to be a combination of both binary complexes. The periodicity of protection in the nucleosome cleavage pattern is preserved but down-weighted by the uniform protection in the TFIIIA-DNA cleavage pattern (Fig. 3).

In order to gain additional insight into the TFIIIA-nucleosome complex, we repeated the hydroxyl radical footprinting experiments with complexes in which the opposite DNA strand (the bottom or "coding" strand) was radioactively end labeled at the *Dde*I site, downstream of the 5S gene (Fig. 1 and 4A). Again, we found that the footprint of the native and tailless nucleosomes in the TFIIIA binding buffer appeared nearly identical, with small differences detected near the edge of the nucleosome footprints (Fig. 4B). In addition, TFIIIA protected nucleotides +39 to +93 from cleavage on the coding strand (Fig. 4A and B, top) as expected (15). It is important to note that the interaction of TFIIIA with the 5S internal promoter is asymmetric, such that the protein appears to interact less intimately with the coding strand than with the noncoding strand (36). Thus, less-extensive protection from DNA cleavage is observed within the TFIIIA footprint in the broad regions that correspond to the binding of fingers 1 to 3 and 7 to 9 (15, 44). Inspection of the gels revealed a pattern of protection that complemented that found for the top (noncoding) strand. The patterns for the ternary complex and the tailless nucleosome were nearly identical from the extreme upstream region to about position +42 (Fig. 4B, Tryp oct/Tern com). As found on the top strand (Fig. 3), this pattern clearly reflects the purely histone-DNA interactions in this region. A similar comparison showed that a portion of the footprint of TFIIIA bound to naked 5S DNA almost exactly matched the hydroxyl radical cleavage pattern of the ternary complex (Fig. 4B, TFIIIA/Tern com). This TFIIIA-like pattern extended from approximately +55 to the extreme downstream positions, corresponding to that observed on the top strand in this region (Fig. 3). Likewise, in between this region and the "histone-like" cleavage pattern in the footprint of the ternary complex lies a transition zone including positions +43 through +57, in which the pattern does not resemble either binary complex alone (Fig. 4). Rather, consistent with the top strand, contacts in this zone have elements of both TFIIIA (most likely the binding of fingers 7 to 9) and histones.

The above results suggest that some histone-DNA interactions are lost when TFIIIA binds to the nucleosome. To address this issue we determined whether histone-DNA contacts near the edge of the internal promoter were maintained or disrupted upon TFIIIA binding to the nucleosome. Nucleosomes were assembled with H2A modified with a photoactivatable cross-linker at amino acid 12. This position is located adjacent to the first α-helix in H2A and lies near the DNA superhelix in the nucleosome core (26), and after brief UV irradiation of these nucleosomes covalent cross-links form between H2A and the noncoding (top) strand of 5S DNA, primarily near position +40 (25). Note that cross-links at this position are located at the very 5′ edge of the TFIIIA binding site and corresponded to a nucleosome translational position with a dyad centered near −3 as expected (Fig. 1) (25). Nucleosomes were reconstituted with the modified H2A and sub-

Downloaded from http://mcb.asm.org/ on July 23, 2019 by guest

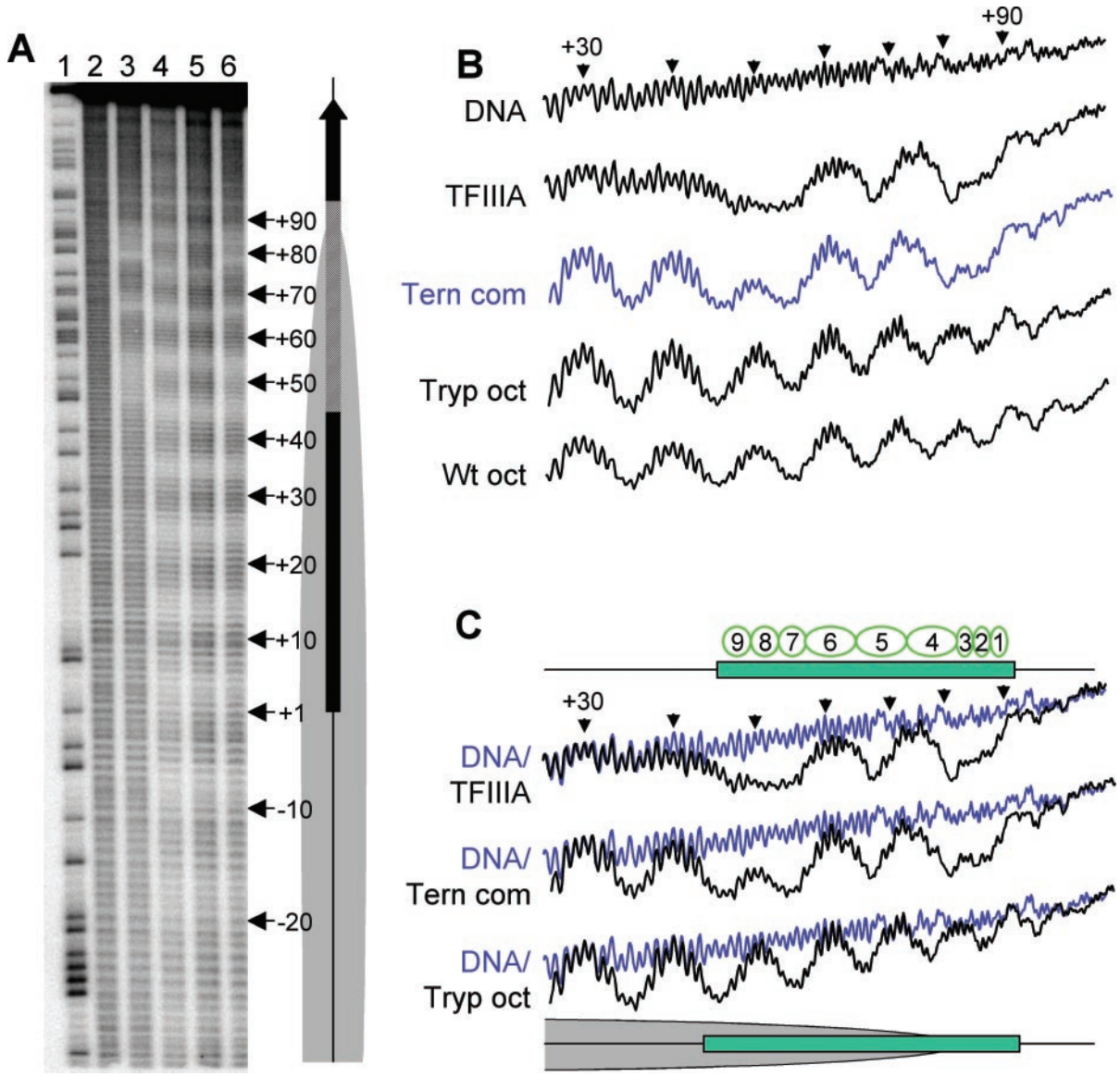

FIG. 2. Hydroxyl radical footprinting of the TFIIIA-5S nucleosome ternary complex. Nucleosomes reconstituted with 5S DNA radiolabeled at the 5′ end of the *Eco*RI site (top strand) and core histones retaining or lacking the tail domains were incubated in the presence or absence of TFIIIA, and then the hydroxyl radical cleavage pattern of the DNA within the resulting complexes was analyzed by denaturing gel electrophoresis and phosphorimagery. (A) Phosphorimage of the cleavage patterns. Lane 1, G-reaction marker; lanes 2 to 6, hydroxyl radical footprints of naked 5S DNA, the TFIIIA-5S DNA complex, native 5S nucleosomes, tailless 5S nucleosomes, and tailless 5S nucleosomes bound by TFIIIA (ternary complex), respectively. (B) Scans of cleavage patterns. Scans were integrated using a window width sufficient to include the entire lane and correspond to the lanes shown in panel A. (C) Comparison of scans of the TFIIIA-DNA complex (TFIIIA), the ternary complex (Tern com), and the tailless nucleosome (Tryp oct) with the naked DNA pattern (DNA; blue line). Regions corresponding to the nucleosome and the internal promoter are indicated.

jected to trypsin proteolysis (Fig. 5A). TFIIIA bound to the tailless APB-modified nucleosomes in a manner similar to nucleosomes containing tailless native histones (Fig. 5B and C). We first determined whether binding of TFIIIA affected the efficiency of histone cross-linking to DNA at this site. We expected that if TFIIIA disrupted histone interactions in the vicinity of the cross-linking site we would detect a net loss of about 50% of the cross-links given the equivalent extent of cross-linking induced by H2A-A12C-APB in both halves of the nucleosome (25). However, we found that an identical yield of cross-link products formed within tailless nucleosomes containing H2A-A12C-APB, whether free or bound by TFIIIA (Fig. 5D). Next, we determined if prior cross-linking between H2A and 5S DNA would have any detectable effect on subsequent TFIIIA binding. Nucleosomes were irradiated to induce cross-linking in approximately 10% of the complexes and then incubated with increasing amounts of TFIIIA. We reasoned that if the presence of a cross-link negatively influenced TFIIIA association, then the protein would preferentially bind un-cross-linked complexes over complexes containing a cross-

Downloaded from http://mcb.asm.org/ on July 23, 2019 by guest

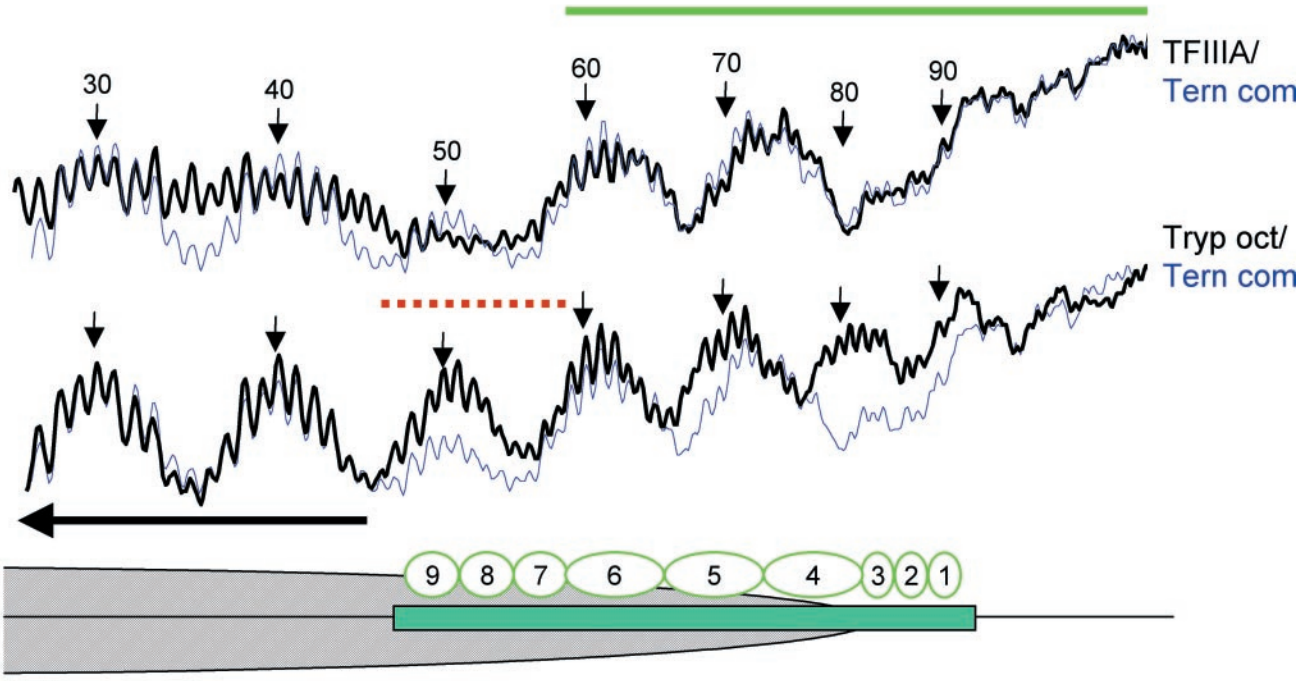

FIG. 3. Both TFIIIA and core histone interactions are detected in the internal promoter of the ternary complex. Top, overlay of scans of the TFIIIA-5S DNA complex (TFIIIA) and the TFIIIA-tailless 5S nucleosome ternary complex (Tern com; blue line). Bottom, overlay of scans of the tailless 5S nucleosome (Tryp oct; black line) and the TFIIIA-tailless 5S nucleosome ternary complex (Tern com; blue line). The green and black horizontal bars indicate regions within the ternary complex that resemble either the TFIIIA-DNA pattern or the nucleosome pattern, respectively. The dashed red bar indicates the transition region in the ternary complex footprint, which resembles both binary complexes.

link, resulting in a reduction of cross-linked species in the TFIIIA-bound compared to unbound nucleosomes. A comparison of the amount of cross-linked species in the TFIIIA-bound and unbound nucleosome bands formed at subsaturating TFIIIA concentrations (Fig. 6A, lane 5) revealed no preference for TFIIIA binding to un-cross-linked versus cross-linked nucleosomes (Fig. 6B, lanes 3 and 4). These results indicate that disruption of histone-DNA interactions in the vicinity of position +40 in the 5S sequence is not required for TFIIIA binding to the nucleosome.

To substantiate the above results, we repeated the experiment with the cross-linker attached to another position within the nucleosome. Recently, Kassabov et al. described a similar cross-linking methodology via position 45 within the histone fold domain of H2A (21). In our hands, nucleosomes containing H2A-A45C modified with APB cross-link to the noncoding (top) strand of 5S DNA at positions +33/+34 and +43/+45 (results not shown), corresponding to the main translational position and perhaps a related position with a dyad at +8 or two cross-link sites from one translational position (6, 34). Nucleosomes assembled with H2A-A45C-APB did not exhibit binding when incubated with increasing amounts of TFIIIA (Fig. 7A), similar to 5S nucleosomes assembled with native histones (17). Likewise, removal of the core histone tail domains greatly stimulated TFIIIA binding (Fig. 7B). Importantly, we found that prior cross-linking of these nucleosomes did not affect subsequent binding of TFIIIA, as equivalent amounts of cross-linked nucleosomes were recovered from free and TFIIIA-bound nucleosomes prepared under subsaturating binding conditions (Fig. 7B and C). These results indicate that disruption of histone-DNA interactions induced by TFIIIA does not extend beyond position +45 in the 5S nucleosome.

In light of our mapping data and the availability of crystal structures for a nucleosome core and the first six fingers of TFIIIA bound to DNA, we constructed a molecular model for the TFIIIA/5S DNA/core histone ternary complex. As mentioned above, our footprinting results indicate that the DNA binding site for fingers 7 to 9 exhibits features of interactions with both TFIIIA as well as core histones. For example, we noted that a peak in the hydroxyl radical cleavage pattern of the 5S nucleosome centered at position +50 (noncoding strand) also occurred (to a lesser extent) in the ternary complex, in the middle of the protected region corresponding to TFIIIA fingers 7 to 9 (Fig. 3). Moreover, our cross-linking results indicated that histone-DNA interactions were not disrupted by TFIIIA binding beyond position +40 to +45. Therefore, we reasoned that both histones and fingers 7 to 9 of TFIIIA might make simultaneous interactions with the DNA in the region +45 to +55. To examine this possibility, we built a molecular model of the ternary complex using the X-ray crystal structure by Nolte et al. of fingers 1 to 6 of TFIIIA bound to a 31-bp DNA fragment from the 5S promoter as a starting point for model building (29). Since we and others have shown that fingers 7 to 9 likely form a similar structural unit as fingers 1 to 3 and interact with DNA in a similar fashion (7, 13, 15), we modeled these fingers onto the end of the model of Nolte et al. to generate a nine-Zn-finger protein bound to 5S

Downloaded from http://mcb.asm.org/ on July 23, 2019 by guest

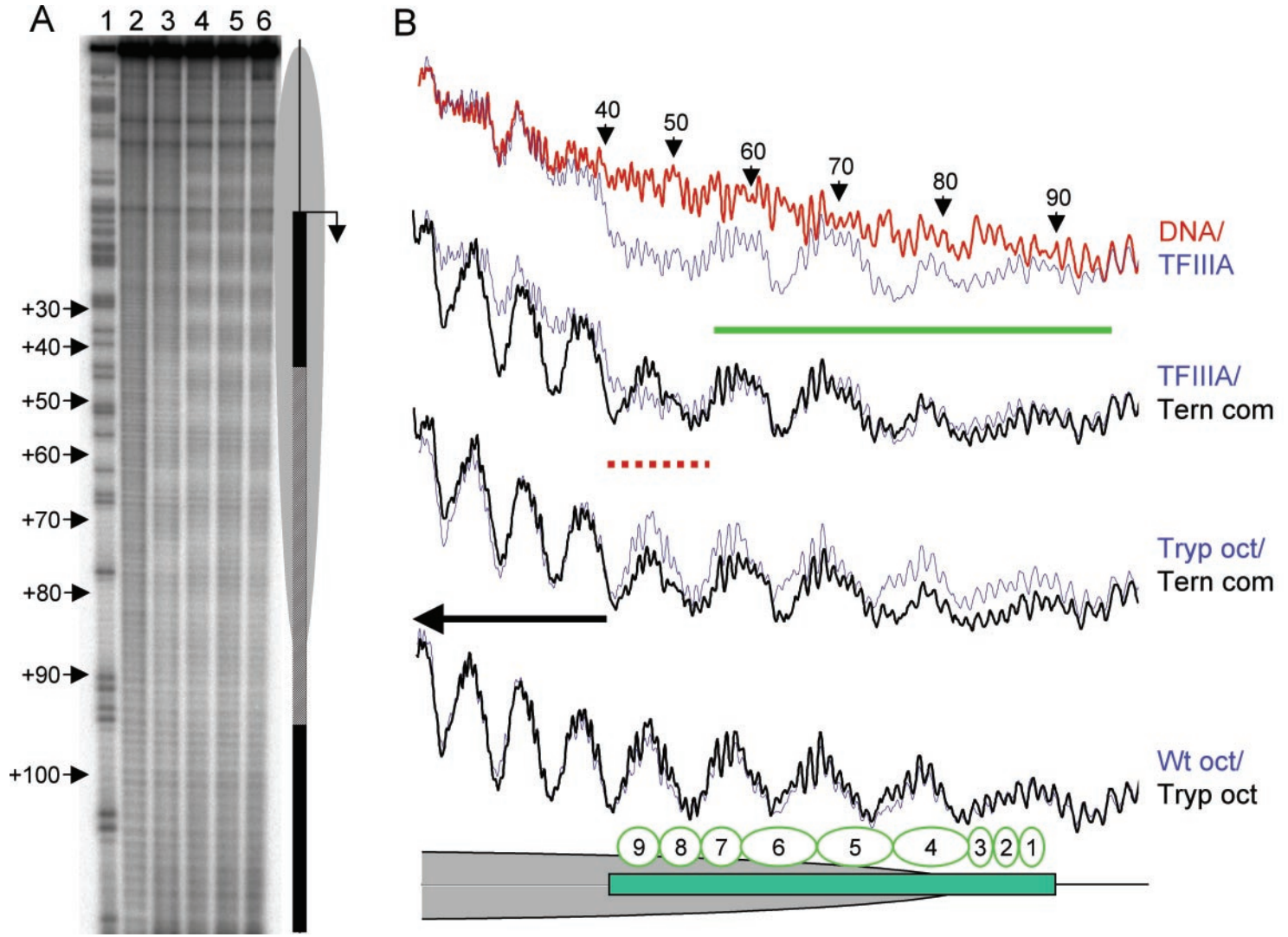

FIG. 4. Hydroxyl radical footprinting of the TFIIIA-5S nucleosome ternary complex. Nucleosomes reconstituted with 5S DNA radiolabeled at the 5′ end of the *Dde*I site (bottom strand) were prepared, and the hydroxyl radical footprints within complexes were analyzed as for Fig. 2. (A) Phosphorimage of the cleavage patterns. Lane 1, G-reaction marker; lanes 2 to 6, hydroxyl radical footprints of naked 5S DNA, the TFIIIA-5S DNA complex, native 5S nucleosomes, tailless 5S nucleosomes, and tailless 5S nucleosomes bound by TFIIIA, respectively. (B) Analysis of scans of naked 5S DNA (DNA; red line), the TFIIIA-DNA complex (TFIIIA; blue line), the ternary complex (Tern com; black line), and the tailless nucleosome (Tryp oct; blue line). Also shown is an overlay of native (Wt oct; blue line) and tailless nucleosomes (Tryp oct; black line). Green, red, and black bars are as described for Fig. 3.

Downloaded from http://mcb.asm.org/ on July 23, 2019 by guest

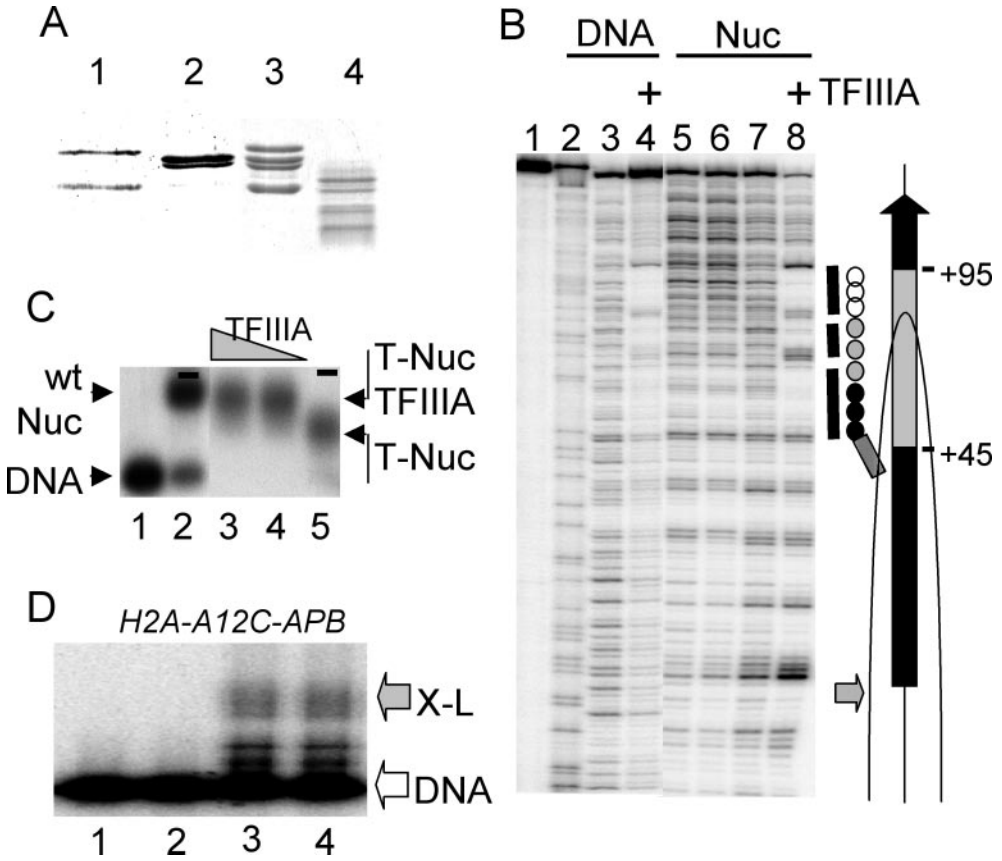

FIG. 5. TFIIIA binding does not affect the interaction between 5S DNA and histone H2A in the 5S nucleosome. Nucleosomes were reconstituted with core histones including H2A-A12C-APB. (A) Protein gel showing native and tailless histones after trypsinolysis. Lanes 1 to 3 show native H3/H4 tetramers, H2A/H2B dimers, and core histone proteins after nucleosome reconstitution, respectively. Lane 4 contains nucleosomal histones after treatment with trypsin to remove tail domains. Note that proteins shown in lanes 2 to 4 include H2A-A12C-APB. (B) The ability of TFIIIA to bind 5S nucleosomes containing intact or tailless H2A-A12C-APB was assessed by DNase I footprinting. Lane 1, uncleaved naked 5S DNA; lane 2, G-reaction marker; lanes 3 and 4, cleavage patterns of the naked 5S DNA fragment in the absence and presence of TFIIIA, respectively; lanes 5 and 6, cleavage patterns of the 5S nucleosome reconstituted with native H2A and H2A-A12C-APB, respectively. Lanes 7 and 8 contain cleavage patterns of the tailless H2A-A12C-APB-containing 5S nucleosome in the absence and presence of TFIIIA, respectively. Graphics at right depict the tripartite footprint (lines) due to binding of the nine Zn fingers of TFIIIA (circles). The transcription activation domain (hatched box) and the location of the nucleosome dyad (horizontal arrow) are shown. The position of the 5S gene and internal promoter are as in Fig. 2. (C) Tailless 5S nucleosomes containing H2A-A12C-APB bind TFIIIA. The tailless 5S nucleosomes were incubated with or without TFIIIA as indicated, and complexes were separated on preparative mobility shift gels. The gels were irradiated, and cross-linking was assessed. (D) Binding of TFIIIA does not affect the efficiency of cross-linking between H2A-A12C-APB and 5S nucleosomal DNA. Radiolabeled DNA from the gel shown in panel C was isolated and separated on an SDS–6% PAGE gel, and cross-linked species were detected by phosphorimager. Lanes 1 and 2, cross-linked products in the naked DNA and native nucleosome bands (panel C, lanes 1 and 2); lanes 3 and 4, cross-linked products in the tailless H2A-A12C-APB nucleosome before and after TFIIIA binding (panel C, lanes 4 and 5).

DNA. We then fit the TFIIIA-DNA complex to the nucleosome model by first precisely aligning the 5S sequence with the model of a nucleosome core particle based on the hydroxyl radical cleavage pattern of the 5S nucleosome (16, 26) (Fig. 2 and 4). This gave residue 116 (in chain I) of the Luger structure as being equivalent to position +40 in the 5S sequence. The nine-Zn-finger structure was then transformed to the appropriate position relative to the nucleosome by first superimposing bp 46 to 48 in the nine-Zn-finger model with the equivalent base pairs (121 to 123) in the Luger structure. We then removed residues downstream of residue 120 in the nucleosomal DNA and "ligated" residue 120 of the Luger structure to residue 46 of the transformed Zn-finger DNA complex. This complex was energy minimized as described in Materials and Methods. The model places fingers 7 to 9 binding to a stretch of DNA also in close proximity and in at least partial contact with the core histone octamer, while fingers 1 to 6 are bound to essentially histone-free DNA. This simultaneous interaction is possible due to the binding of fingers 7 to 9 to a face of the nucleosomal DNA that is not in contact with the core histones. Note that due to constraints of model construction, it was necessary to model fingers 7 to 9 as being completely associated with DNA, in a manner identical to that of fingers 1 to 3. However, our footprinting data suggest that these fingers may not bind in a completely unrestricted fashion. In addition, the orientation of TFIIIA in our model predicted that the 4-kDa COOH-terminal transcription-activation domain would likely extend away from the complex, in position to interact with TFIIIC (11, 22) (see below).

Downloaded from http://mcb.asm.org/ on July 23, 2019 by guest

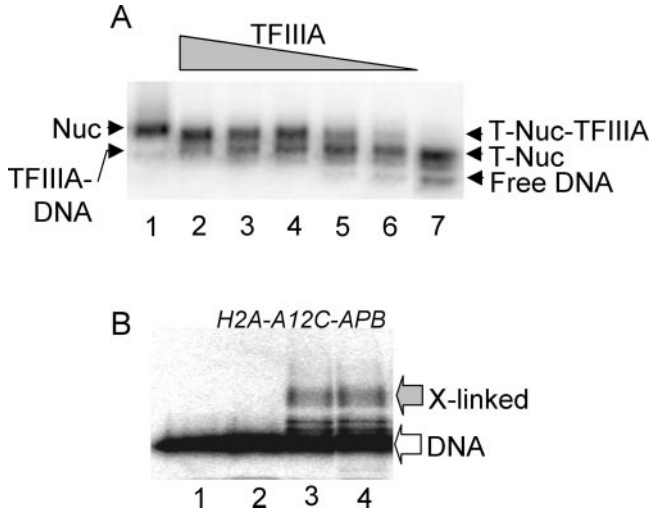

FIG. 6. Prior cross-linking between H2A-A12C-APB and 5S nucleosome DNA does not affect binding of TFIIIA. Tailless 5S nucleosomes containing H2A-A12C-APB were first irradiated, and then the ability of TFIIIA to bind cross-linked nucleosomes was assessed. (A) Preparative nucleoprotein gel. Lane 1, native 5S nucleosomes (Nuc); lanes 2 to 7, tailless 5S nucleosomes containing APB-H2A-A12C (T-Nuc) incubated with decreasing amounts of TFIIIA or without TFIIIA. (B) TFIIIA readily binds cross-linked nucleosomes. Cross-linking within various species shown in panel A was assessed on SDS–6% PAGE gels as in Fig. 5D. Lanes 1 and 2, cross-linking within naked 5S DNA and native 5S nucleosomes lacking an APB modification (panel A, lanes 7 and 1, respectively). Lanes 3 and 4, cross-linked species in the tailless 5S nucleosomes unbound or bound by TFIIIA (panel A, lane 7 and lane 5 upper band, respectively).

DISCUSSION

Our analysis of the TFIIIA/DNA/histone ternary complex provides a picture of an important initial intermediate on the pathway from naïve chromatin structure to productive polymerase (pol) III transcription complex. This transition is initiated by the invasion of the nucleosome structure by the binding of a portion of TFIIIA to the 5S internal promoter. TFIIIA binding is initiated from the 3′ (downstream) end of the internal promoter and involves the N-terminal Zn-finger domains of the protein, where the energetically most significant protein-DNA contacts are located (7, 15, 36). However, we found that binding apparently did not proceed to complete association of all nine Zn fingers of TFIIIA and close association of the COOH-terminal transcription-activation domain with DNA. Indeed, substantial histone-DNA interactions were detected in the region of the binding site corresponding to fingers 7 to 9 (Fig. 3 and 4B). Moreover, the portion of the footprint contributed by the C-terminal domain of TFIIIA was not apparent in the cleavage pattern of the ternary complex. Previously reported contacts for Zn fingers 7 to 9 end abruptly at +49 on the top (noncoding) strand; however, the footprint of the full-length protein extends to position +42 on this strand, presumably due to additional protection afforded by the C-terminal domain of TFIIIA (13). The pattern for the triple complex in this region clearly represents only histone-DNA interactions, suggesting that the C-terminal domain of TFIIIA is no longer in close proximity to the nucleosomal DNA, perhaps due to the continued bending of DNA around the histones in this region.

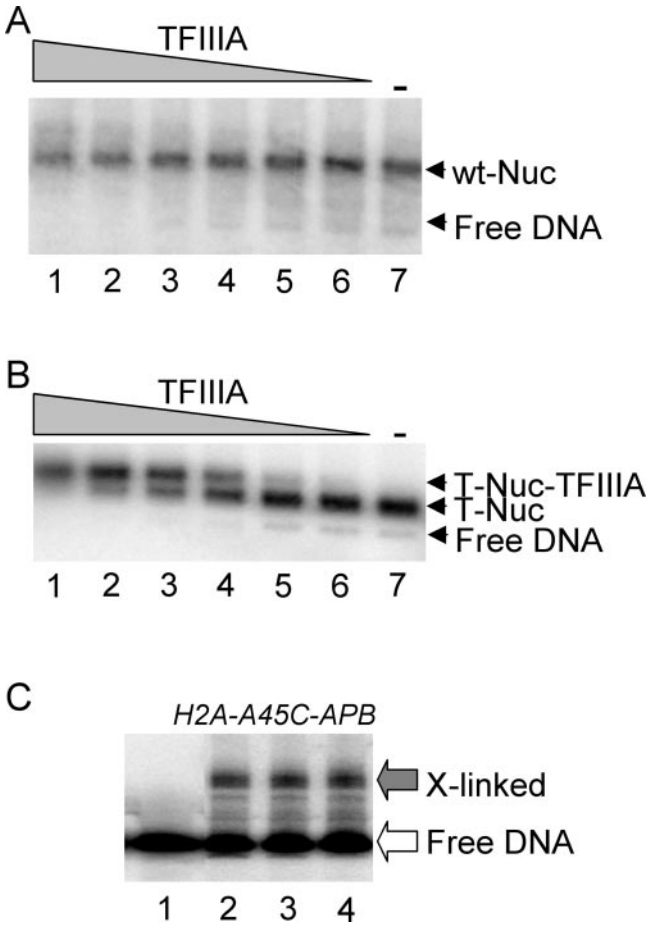

FIG. 7. TFIIIA binding does not disrupt interaction between 5S DNA and the histone fold domain in H2A in the 5S nucleosome. Nucleosomes were reconstituted with core histones including H2A-A45C-APB, and then tail domains were removed from a portion of the sample by trypsin proteolysis. (A and B) Binding of TFIIIA to native (A) or tailless (B) 5S nucleosomes containing H2A-A45C-APB. Lanes 1 to 6, nucleosomes incubated with decreasing amounts of TFIIIA; lane 7, nucleosomes incubated without TFIIIA. The gels were irradiated, and cross-linking was assessed. (C) Binding of TFIIIA does not affect the efficiency of cross-linking between H2A-A45C-APB and 5S nucleosomal DNA. Radiolabeled DNA from bands in the gel shown in panel B was isolated and separated on an SDS–6% PAGE gel, and cross-linked species were detected by phosphorimager. Lane 1, naked 5S DNA (panel B, lane 2); lane 7, DNA from nucleosomes incubated in the absence of TFIIIA (panel B, lane 7); lanes 3 and 4, DNA from nucleosomes remaining unbound or bound by TFIIIA (panel B, lane 4, top and bottom bands, respectively).

We also note that binding of TFIIIA to the nucleosome does not result in displacement of an H2A/H2B dimer (43), suggesting that DNA unwrapping does not occur past the dimer-tetramer junction near position +30 in the 5S sequence. These observations and results from the cross-linking experiments support the notion that DNA in the +45 to +55 region is in contact with histone proteins as well as fingers 7 to 9 of TFIIIA.

It is possible that complete binding of TFIIIA and disruption of the remaining histone-DNA interactions in the internal promoter require binding of the pol III factors TFIIIC and TFIIIB. On naked DNA, the TFIIIA-DNA complex nucleates

Downloaded from http://mcb.asm.org/ on July 23, 2019 by guest

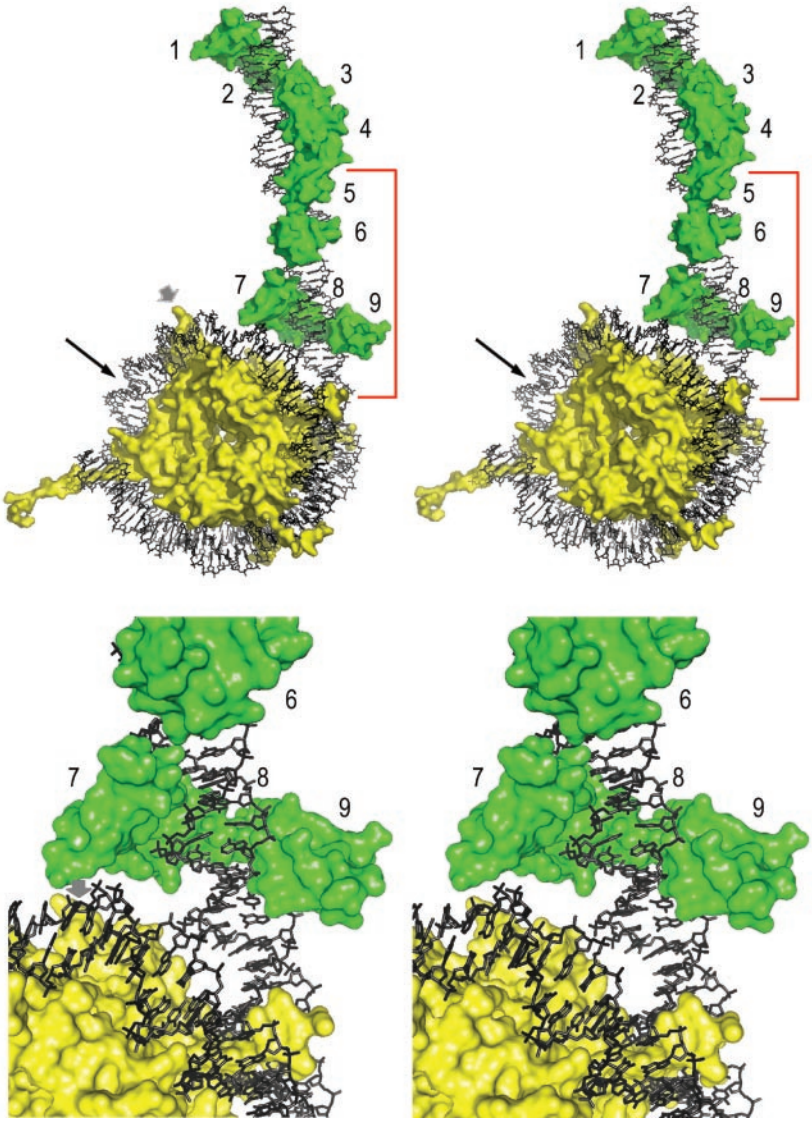

FIG. 8. Model of the TFIIIA/5S DNA/core histone ternary complex. Stereoviews of the model show TFIIIA (green), DNA (black lines), and the core histone octamer (yellow). Individual fingers are labeled. The bracket indicates the region of DNA unwrapped from the histone surface upon TFIIIA binding. The arrow indicates the approximate position of the nucleosome dyad. The locations of the base of the H3 and H4 tail domains nearest the TFIIIA binding site are indicated by gray arrows in the top and bottom views, respectively.

binding of transcription factors IIIC and IIIB to form a stable preinitiation complex which includes contacts throughout the 5S gene and some extragenic sequences (22, 50). Binding of TFIIIC stabilizes association of TFIIIA in a manner dependent upon the COOH-terminal transcription activation domain (11, 47). While the TFIIIC-dependent stabilization apparently does not change the TFIIIA-DNA footprint on naked DNA (11), the subsequent association of TFIIIB to complete the preinitiation complex leads to a drastic increase in the extent of protein interaction throughout the 5S gene (50). Future hydroxyl radical footprinting and cross-linking analyses involving TFIIIC and TFIIIB will shed light on intermediates to preinitiation complex formation on chromatin templates.

The observation that acetylation or removal of the core histone tail domains greatly stimulates TFIIIA binding to the 5S nucleosome (23, 43) correlates with the fact that transcriptionally active 5S genes are acetylated in vivo (19). Indeed, the initial invasion of the nucleosome by TFIIIA may require this modification; however, the basis of this stimulation remains unclear. As mentioned above, acetylation results in only modest enhancements in the probability of DNA unwrapping from the 5S nucleosome (6), consistent with results obtained with nucleosomes assembled with other DNA sequences (31). Binding does not alter the stoichiometry of core histones within the nucleosome or result in significant changes in the breadth of histone-DNA interactions (2, 12, 43). It is interesting that trypsin removes 11, 23, 26, and 17 or 19 amino acids from H2A, H2B, H3, and H4 N termini, respectively (42). By comparison, approximately 10, 26, 37, and 15 residues within each tail project beyond the perimeter of the DNA superhelix in the

Downloaded from http://mcb.asm.org/ on July 23, 2019 by guest

nucleosome (11 and 9 for the H2A C terminus). Thus, while acetylated lysines are removed by trypsin, the degree to which tail removal mechanistically resembles acetylation vis-à-vis stimulation of TFIIIA binding is not known. Finally, while it is possible that acetylation or removal of the tails increases mobility of the nucleosome, our cross-linking studies suggested that nucleosome mobilization is not required for TFIIIA binding (Fig. 6).

An alternative possibility is that the unmodified tails directly interfere with TFIIIA binding. Our modeling study suggested that TFIIIA is positioned such that its C-terminal domain is oriented away from the core histone octamer, but in the vicinity of the core histone tail domains. Nonetheless, it is formally possible that the C-terminal domain could make counterproductive interactions with some of the tail domains or otherwise encounter steric interference from these domains, leading to a drastic loss of the ability of TFIIIA to bind its site in the nucleosome. Experiments are in progress to test the role of the COOH-domain in restricting access of TFIIIA to the 5S nucleosome.

Utilizing the data reported here as well as previously reported results, we constructed a detailed model of the TFIIIA/5S DNA/histone octamer ternary complex (Fig. 8). The model provides a structural basis for understanding the complex pattern associated with the transition zone between the TFIIIA-like and nucleosome-like portions of the hydroxyl radical footprint of the ternary complex. The hydroxyl radical footprint for this region (+49 to +59) exhibits elements of both histone-DNA and TFIIIA-DNA interactions. Our model shows that it is sterically possible for TFIIIA Zn fingers 7 to 9 to be in close proximity to the DNA helix in this region, while the DNA itself is in near contact with the histone surface, thus accounting for the complex hydroxyl radical cleavage pattern. Note that while our model necessarily portrays fingers 7 to 9 in full contact with the DNA (Fig. 4), it is possible that these fingers are only partially engaged with DNA or in equilibrium with a state in which the fingers are partially bound. Interestingly, as mentioned above, close apposition of the C-terminal transcription activation domain and 5S DNA, evident in the footprint of the TFIIIA/5S DNA complex, was not evident in the ternary complex. Accordingly, our model suggests that this domain projects away from the nucleosome in the ternary complex, perhaps due to the curvature of the DNA in the +42 to +49 region. This exposure may actually facilitate the binding of TFIIIC to this domain, perhaps promoting further disruption of histone-DNA interactions on the pathway to formation of a complete preinitiation complex.

ACKNOWLEDGMENTS

We thank C. Zheng for mutant histone proteins.

This work was supported by National Institutes of Health grant RO1GM52426. R.B. is a Research Scholar of the Leukemia and Lymphoma Society of America.

REFERENCES

1. **Almouzni, G., M. Mechali, and A. P. Wolffe.** 1990. Competition between transcription complex assembly and chromatin assembly on replicating DNA. EMBO J. **9:**573–582.
2. **Bauer, W. R., J. J. Hayes, J. H. White, and A. P. Wolffe.** 1994. Nucleosome structural changes due to acetylation. J. Mol. Biol. **236:**685–690.
3. **Bouvet, P., S. Dimitrov, and A. P. Wolffe.** 1994. Specific regulation of Xenopus chromosomal 5S rRNA gene transcription in vivo by histone H1. Genes Dev. **8:**1147–1159.
4. **Brown, R. S., C. Sander, and A. P. Wolffe.** 1985. The primary structure of transcription factor TFIIIA has 12 consecutive repeats. FEBS Lett. **186:**271–274.
5. **Brunger, A., P. Adams, G. Clore, W. DeLano, P. Gros, R. Grosse-Kunstleve, J. Jiang, J. Kuszewski, M. Nilges, N. Pannu, R. Read, L. Rice, T. Simonson, and G. Warren.** 1998. Crystallography & NMR system: a new software suite for macromolecular structure determination. Acta Crystallogr. D **54:**905–921.
6. **Chafin, D. R., J. M. Vitolo, L. A. Henricksen, R. A. Bambara, and J. J. Hayes.** 2000. Human DNA ligase I efficiently seals nicks in nucleosomes. EMBO J. **19:**5492–5501.
7. **Clemens, K. R., X. Liao, V. Wolf, P. E. Wright, and J. M. Gottesfeld.** 1992. Definition of the binding sites of individual Zn-fingers in the transcription factor IIIA-5S RNA gene complex. Proc. Natl. Acad. Sci. USA **89:**10822–10826.
8. **Del Rio, S., and D. R. Setzer.** 1991. High yield purification of active transcription factor IIIA expressed in E. coli. Nucleic Acids Res. **19:**6197–6203.
9. **Engelke, D. R., S.-Y. Ng, B. S. Shastry, and R. G. Roeder.** 1980. Specific interaction of a purified transcription factor with an internal control region of 5S RNA genes. Cell **19:**717–728.
10. **Gottesfeld, J. M.** 1987. DNA sequence-directed nucleosome reconstitution on 5S RNA genes of *Xenopus laevis*. Mol. Cell. Biol. **7:**1612–1622.
11. **Hayes, J., T. D. Tullius, and A. P. Wolffe.** 1989. A protein-protein interaction is essential for stable complex formation on a 5S RNA gene. J. Biol. Chem. **264:**6009–6012.
12. **Hayes, J. J., D. J. Clark, and A. P. Wolffe.** 1991. Histone contributions to the structure of DNA in the nucleosome. Proc. Natl. Acad. Sci. USA **88:**6829–6833.
13. **Hayes, J. J., and K. R. Clemens.** 1992. Location of contacts between individual zinc fingers of Xenopus laevis transcription factor IIIA and the internal control region of a 5S RNA gene. Biochemistry **31:**11600–11605.
14. **Hayes, J. J., and K. M. Lee.** 1997. In vitro reconstitution and analysis of mononucleosomes containing defined DNAs and proteins. Methods **12:**2–9.
15. **Hayes, J. J., and T. D. Tullius.** 1992. The structure of the TFIIIA/5S DNA complex. J. Mol. Biol. **227:**407–417.
16. **Hayes, J. J., T. D. Tullius, and A. P. Wolffe.** 1990. The structure of DNA in a nucleosome. Proc. Natl. Acad. Sci. USA **87:**7405–7409.
17. **Hayes, J. J., and A. P. Wolffe.** 1992. Histones H2A/H2B inhibit the interaction of transcription factor IIIA with the Xenopus borealis somatic 5S RNA gene in a nucleosome. Proc. Natl. Acad. Sci. USA **89:**1229–1233.
18. **Hayes, J. J., and A. P. Wolffe.** 1992. The interaction of transcription factors with nucleosomal DNA. Bioessays **14:**597–603.
19. **Howe, L., T. A. Ranalli, C. D. Allis, and J. Ausio.** 1998. Transcriptionally active Xenopus laevis somatic 5S ribosomal RNA genes are packaged with hyperacetylated histone H4, whereas transcriptionally silent oocyte genes are not. J. Biol. Chem. **273:**20693–20696.
20. **Jones, T., J. Zou, S. Cowan, and M. Kjeldgaard.** 1991. Improved methods for building protein models in electron density maps and the location of errors in these models. Acta Crystallogr. A **47:**110–119.
21. **Kassabov, S. R., N. M. Henry, M. Zofall, T. Tsukiyama, and B. Bartholomew.** 2002. High-resolution mapping of changes in histone-DNA contacts of nucleosomes remodeled by ISW2. Mol. Cell. Biol. **22:**7524–7534.
22. **Lassar, A. B., P. L. Martin, and R. G. Roeder.** 1983. Transcription of class III genes: formation of preinitiation complexes. Science **222:**740–748.
23. **Lee, D. Y., J. J. Hayes, D. Pruss, and A. P. Wolffe.** 1993. A positive role for histone acetylation in transcription factor access to nucleosomal DNA. Cell **72:**73–84.
24. **Lee, K. M., D. R. Chafin, and J. J. Hayes.** 1999. Targeted cross-linking and DNA cleavage within model chromatin complexes. Methods Enzymol. **304:**231–251.
25. **Lee, K. M., and J. J. Hayes.** 1997. The N-terminal tail of histone H2A binds to two distinct sites within the nucleosome core. Proc. Natl. Acad. Sci. USA **94:**8959–8964.
26. **Luger, K., A. W. Mader, R. K. Richmond, D. F. Sargent, and T. J. Richmond.** 1997. Crystal structure of the nucleosome core particle at 2.8 Å resolution. Nature **389:**251–260.
27. **Miller, J., A. D. McLachlan, and A. Klug.** 1985. Repetitive zinc-binding domains in the protein transcription factor IIIA from Xenopus oocytes. EMBO J. **4:**1609–1614.
28. **Miller, J. A., and J. Widom.** 2003. Collaborative competition mechanism for gene activation in vivo. Mol. Cell. Biol. **23:**1623–1632.
29. **Nolte, R. T., R. M. Conlin, S. C. Harrison, and R. S. Brown.** 1998. Differing roles for zinc fingers in DNA recognition: structure of a six-finger transcription factor IIIA complex. Proc. Natl. Acad. Sci. USA **95:**2938–2943.
30. **Pavletich, N. P., and C. O. Pabo.** 1993. Crystal structure of a five-finger GLI-DNA complex: new perspectives on zinc fingers. Science **261:**1701–1707.
31. **Polach, K. J., P. T. Lowary, and J. Widom.** 2000. Effects of core histone tail domains on the equilibrium constants for dynamic DNA site accessibility in nucleosomes. J. Mol. Biol. **298:**211–233.
32. **Polach, K. J., and J. Widom.** 1995. Mechanism of protein access to specific

Downloaded from http://mcb.asm.org/ on July 23, 2019 by guest

DNA sequences in chromatin: a dynamic equilibrium model for gene regulation. J. Mol. Biol. **254:**130–149.
33. **Polach, K. J., and J. Widom.** 1996. A model for the cooperative binding of eukaryotic regulatory proteins to nucleosomal target sites. J. Mol. Biol. **258:**800–812.
34. **Pruss, D., B. Bartholomew, J. Persinger, J. Hayes, G. Arents, E. N. Moudrianakis, and A. P. Wolffe.** 1996. An asymmetric model for the nucleosome: a binding site for linker histones inside the DNA gyres. Science **274:**614–617.
35. **Rhodes, D.** 1985. Structural analysis of a triple complex between the histone octamer, a Xenopus gene for 5S RNA and transcription factor IIIA. EMBO J. **4:**3473–3482.
36. **Sakonju, S., and D. D. Brown.** 1982. Contact points between a positive transcription factor and the Xenopus 5S RNA gene. Cell **31:**395–405.
37. **Simon, R. H., and G. Felsenfeld.** 1979. A new procedure for purifying histone pairs H2A + H2B and H3 + H4 from chromatin using hydroxylapatite. Nucleic Acids Res. **6:**689–696.
38. **Simpson, R. T.** 1991. Nucleosome positioning: occurrence, mechanisms, and functional consequences. Prog. Nucleic Acid Res. Mol. Biol. **40:**143–184.
39. **Smith, D. R., I. J. Jackson, and D. D. Brown.** 1984. Domains of the positive transcription factor specific for the Xenopus 5S RNA gene. Cell **37:**645–652.
40. **Thiriet, C., and J. J. Hayes.** 1998. Functionally relevant histone-DNA interactions extend beyond the classically defined nucleosome core region. J. Biol. Chem. **273:**21352–21358.
41. **Tse, C., and J. C. Hansen.** 1997. Hybrid trypsinized nucleosomal arrays: identification of multiple functional roles of the H2A/H2B and H3/H4 N-termini in chromatin fiber compaction. Biochemistry **36:**11381–11388.
42. **van Holde, K. E.** 1989. Chromatin. Springer Verlag, New York, N.Y.
43. **Vitolo, J. M., C. Thiriet, and J. J. Hayes.** 2000. The H3-H4 N-terminal tail domains are the primary mediators of transcription factor IIIA access to 5S DNA within a nucleosome. Mol. Cell. Biol. **20:**2167–2175.
44. **Vrana, K. E., M. E. Churchill, T. D. Tullius, and D. D. Brown.** 1988. Mapping functional regions of transcription factor TFIIIA. Mol. Cell. Biol. **8:**1684–1696.
45. **Wolfe, S. A., L. Nekludova, and C. O. Pabo.** 2000. DNA recognition by Cys2His2 zinc finger proteins. Annu. Rev. Biophys. Biomol. Struct. **29:**183–212.
46. **Wolffe, A. P.** 1998. Chromatin structure and function, 3rd ed. Academic Press, San Diego, Calif.
47. **Wolffe, A. P.** 1988. Transcription fraction TFIIIC can regulate differential Xenopus 5S RNA gene transcription in vitro. EMBO J. **7:**1071–1079.
48. **Wolffe, A. P., and D. D. Brown.** 1988. Developmental regulation of two 5S ribosomal RNA genes. Science **241:**1626–1632.
49. **Wolffe, A. P., and J. J. Hayes.** 1999. Chromatin disruption and modification. Nucleic Acids Res. **27:**711–720.
50. **Wolffe, A. P., and R. H. Morse.** 1990. The transcription complex of the Xenopus somatic 5 S RNA gene. A functional analysis of protein-DNA interactions outside of the internal control region. J. Biol. Chem. **265:**4592–4599.
51. **Wuttke, D. S., M. P. Foster, D. A. Case, J. M. Gottesfeld, and P. E. Wright.** 1997. Solution structure of the first three zinc fingers of TFIIIA bound to the cognate DNA sequence: determinants of affinity and sequence specificity. J. Mol. Biol. **273:**183–206.
52. **Zheng, C., and J. J. Hayes.** 2003. Intra- and inter-nucleosomal protein-DNA interactions of the core histone tail domains in a model system. J. Biol. Chem. **278:**24217–24224.

Downloaded from http://mcb.asm.org/ on July 23, 2019 by guest